Biochimica et Biophysica Acta 1807 (2011) 270–274

Contents lists available at ScienceDirect

Biochimica et Biophysica Acta

journal homepage: www.elsevier.com/locate/bbabio

Regional variation in mitochondrial DNA copy number in mouse brain

Satoshi Fuke [a], Mie Kubota-Sakashita [a], Takaoki Kasahara [a], Yasufumi Shigeyoshi [b], Tadafumi Kato [a,*]

[a] Laboratory for Molecular Dynamics of Mental Disorders, RIKEN Brain Science Institute, 2-1 Hirosawa, Wako, Saitama 351-0198, Japan
[b] Department of Anatomy and Neurobiology, Kinki University School of Medicine, 377-2 Ohno-Higashi, Osakasayama, Osaka 589-8511, Japan

ARTICLE INFO

Article history:
Received 3 August 2010
Received in revised form 10 November 2010
Accepted 30 November 2010
Available online 8 December 2010

Keywords:
Cerebellum
Copy number
Dopamine
mtDNA
Substantia nigra
Ventral tegmental area

ABSTRACT

Mitochondria have their own DNA (mitochondrial DNA [mtDNA]). Although mtDNA copy number is dependent on tissues and its decrease is associated with various neuromuscular diseases, detailed distribution of mtDNA copies in the brain remains uncertain. Using real-time quantitative PCR assay, we examined regional variation in mtDNA copy number in 39 brain regions of male mice. A significant regional difference in mtDNA copy number was observed ($P<4.8\times10^{-35}$). High levels of mtDNA copies were found in the ventral tegmental area and substantia nigra, two major nuclei containing dopaminergic neurons. In contrast, cerebellar vermis and lobes had significantly lower copy numbers than other regions. Hippocampal dentate gyrus also had a relatively low mtDNA copy number. This study is the first quantitative analysis of regional variation in mtDNA copy number in mouse brain. Our findings are important for the physiological and pathophysiological studies of mtDNA in the brain.

1. Introduction

Mitochondria play important roles in energy production, apoptosis, calcium signaling, as well as synaptic transmission, and neuroplasticity in neurons [1]. Mitochondrial dysfunction induces various mitochondrial diseases and may also be linked to neurodegenerative disorders, such as Parkinson's disease (PD), Alzheimer's disease, and Huntington's disease [2–4]. These mitochondrial dysfunctions can result from heteroplasmic mitochondrial DNA (mtDNA) mutations, including point mutations and deletions in mtDNA [4,5]. A mitochondrion contains a number of mtDNA copies, and mtDNA depletion also causes mitochondrial diseases [5–10]. It is possible that differences in mtDNA copy number among brain regions lead to association with region-dependent mitochondrial function and disease susceptibility. However, the distribution of mtDNA copies in the brain has not been studied in detail so far.

In the present study, we determined mtDNA copy number in 39 representative brain regions of adult mice using a micropunch technique and real-time quantitative PCR (qPCR). The results demonstrate that mtDNA is enriched in substantia nigra (SN) and the ventral tegmental area (VTA), where dopaminergic neurons are located.

2. Materials and methods

2.1. Animals

Male C57BL/6J mice were kept in the laboratory under light/dark conditions of 12 h:12 h (lights on at 8:00 a.m.). The laboratory was air-conditioned, and temperature and humidity were maintained at approximately 22–23 °C and 50–60%, respectively. From age 20 to 28 weeks, mice were individually housed in cages (24 cm wide × 11 cm deep × 14 cm high) equipped with a steel wheel (5 cm wide × 14 cm in diameter). All animal experiments were performed in accordance with the protocols approved by the Animal Experiment Committee of RIKEN (Wako, Saitama, Japan). All efforts were made to minimize the number of animals used and their suffering.

2.2. Micropunch

Transcardiac perfusion fixation was performed with 4% paraformaldehyde in phosphate-buffered saline (PBS), and then brains were immersed in PBS.

Slices (0.5 mm thick) of mouse brain were generated using a mouse brain matrix (Neuroscience, Tokyo, Japan), and 39 regions (Table 1, Fig. 1) were punched out bilaterally from the fixed slices under a stereomicroscope with a handmade microdissecting needle (gauge 0.5 mm), which has thinner wall than commercially available micropunchers, to pick up adjacent regions from one slice. The anatomical nomenclature is based on the atlas of Franklin and Paxinos

* Corresponding author. Tel.: +81 48 467 6949; fax: +81 48 467 6947.
E-mail address: kato@brain.riken.jp (T. Kato).

0005-2728/$ – see front matter © 2010 Elsevier B.V. All rights reserved.
doi:10.1016/j.bbabio.2010.11.016

Table 1
Micropunched 39 brain regions.

Brain area	Abbreviations	Brain region
Cerebral cortex	PrL-s	Prelimbic cortex–superficial layers
	PrL-de	Prelimbic cortex–deep layers
	IL-s	Infralimbic cortex–superficial layers
	IL-de	Infralimbic cortex–deep layers
	Cg	Cingulate cortex
	Motor-s	Motor cortex–superficial layers
	Motor-in	Motor cortex–intermediate layers
	Motor-de	Motor cortex–deep layers
	cc	Corpus callosum
Hippocampus	CA1	CA1
	CA2/CA3	CA2, CA3
	DG	Dentate gyrus
Amygdala	A Amy-m	Anterior amygdaloid complex–medial
	A Amy-l	Anterior amygdaloid complex–lateral
	P Amy-m	Posterior amygdaloid complex–medial
	P Amy-l	Posterior amygdaloid complex–lateral
Septum	LS	Lateral septal nucleus
Basal ganglia	Acb-core	Accumbens nucleus–core
	Acb-shell	Accumbens nucleus–shell
	CP-m	Caudate putamen–medial
	CP-l	Caudate putamen–lateral
	LGP	Lateral globus pallidus
Thalamus	VP	Ventral posterior thalamic nucleus
	PVT	Paraventricular nucleus of thalamus
	MD	Mediodorsal thalamic nucleus
	Hb	Habenular nucleus
	LG	Lateral geniculate body
	MG	Medial geniculate body
Hypothalamus	SCN	Suprachiasmatic nucleus
	SPZ-v	Subparaventricular zone–ventral part
	SPZ-do	Subparaventricular zone–dorsal part
	PV	Paraventricular hypothalamic nucleus
	LH	Lateral hypothalamic area
Midbrain	SN	Substantia nigra
	VTA	Ventral tegmental area
	IP	Interpeduncular nucleus
	PAG	Periaqueductal gray
Cerebellum	Cb-vermis	Cerebellar cortex–vermis
	Cb-lobe	Cerebellar cortex–lobe

(Fig. 1) [11]. After overnight incubation of each micropunched region in lysis buffer (1 punch/25 μl, 10 mM Tris–HCl, pH 8.0, 1 mM EDTA, pH 8.0, 0.5% Triton X-100, and 500 μg/ml proteinase K [Roche Applied Science, Mannheim, Germany]) at 55 °C, samples were incubated at 65 °C over 6 h to de-crosslink, followed by heat inactivation at 96 °C for 10 min and addition of an equal amount of 10 mM Tris–HCl (pH 8.0).

2.3. Real-time qPCR analysis

Real-time qPCR analysis was performed using the 7900HT Fast Real-Time PCR System (Applied Biosystems, Foster City, CA, USA) with SYBR Premix Ex Taq reagent (Takara Bio, Otsu, Japan) according to the manufacturer's instructions. Each PCR product was separately amplified from 2 μl of lysate of micropunched sample in a 10-μl reaction containing 5 μl of 2 × SYBR Premix and 0.2 μM of each primer.

For estimation of amounts of mtDNA in mice, the control region (D-loop) of mouse mtDNA was amplified using the primer pair D1 (5′-CCC AAG CAT ATA AGC TAG TAC-3′) and D2 (5′-ATA TAA GTC ATA TTT TGG GAA CTA C-3′). Using this primer set, the thermal cycling protocol used was 95 °C for 20 s, 55 °C for 20 s, 72 °C for 80 s for 30 cycles after an initial denaturation. In a preliminary experiment, the quantification using *COX1* or *ND4* region in mtDNA showed similar results to quantification using D-loop region, that is, lower copy number in cerebellum compared with frontal lobe, other cortices, and basal ganglia (Supplementary Figure 1). For determination of the amount of nuclear DNA, the *apoB* gene was used as a reference: 5′-CGT GGG CTC CAG CAT TCT A-3′ and 5′-TCA CCA GTC ATT TCT GCC TTT G-3′. In the case of amplification using these three primer sets, 40 cycles of two-step PCR followed: 95 °C for 10 s and 60 °C for 30 s after an initial denaturation at 95 °C for 1 min.

These real-time qPCRs were carried out in quadruplicate for all measurements. After confirmation of the single major peak representing the specific amplification with the melting curve, the quantities of each PCR product were calibrated by a linear regression model, using standard curves calculated between Ct values and the logarithm of concentrations of standard pCR2.1-TOPO plasmids (Invitrogen, Carlsbad, CA, USA) containing each PCR fragment. In every run, the high linearity (R^2>0.99) of the standard curves was verified by amplifications of each PCR product from dilution series of the plasmids made up to 10 ng by pCR2.1-TOPO plasmid. Ct values of all samples were within the linear range.

The relative number of mtDNA copies per cell was calculated as the normalized ratio of D-loop/*apoB* gene to a median value of 39 brain regions. In all samples examined, PCR products both of the D-loop in mtDNA and of the *apoB* gene in nuclear genome were amplified within the linear range of assays.

2.4. Statistical analysis

The results of quantitative experiments were analyzed by nonparametric tests after use of the Kolmogorov–Smirnov test for confirmation of a normal distribution. A two-tailed test was used for exploratory analysis. Statistical significance was determined using KyPlot 4.0 (KyensLab, Tokyo, Japan). Relative mtDNA copy numbers in several regions did not show a statistically normal distribution (Kolmogorov–Smirnov test, $P<0.05$). Therefore, we used nonparametric tests for detection of statistical significance among brain regions. To determine detailed significant regional differences in mtDNA copy number, we used the nonparametric multiple comparison Steel–Dwass test ($\alpha = 0.05$).

3. Results

The average relative mtDNA copy number in the 39 brain areas was between 0.0847 and 2.54 (Fig. 1). There was a statistically significant regional variation in mtDNA copy number among the 39 brain regions (Kruskal–Wallis test, $P<4.8\times10^{-35}$) (Fig. 2). In VTA, the mtDNA copy number (median = 2.62, average ± SD = 2.54 ± 0.80) was significantly higher than in 24 other regions. The relative mtDNA copy number in SN (median = 2.12, average ± SD = 2.23 ± 0.65) was higher than in 19 other regions. Moreover, the interpeduncular nucleus (IP) showed a significantly higher mtDNA copy number (median = 1.76, average ± SD = 1.86 ± 0.53) than did 14 other brain regions.

In contrast, a significantly lower mtDNA copy number was observed in the anterior cerebellar lobe (Cb-lobe) (median = 0.0965, average ± SD = 0.0847 ± 0.0492) than in most other regions. MtDNA copy number in cerebellar vermis (Cb-vermis) (median = 0.0857, average ± SD = 0.144 ± 0.157) was lower than in 28 other brain regions. In the dentate gyrus (DG), mtDNA copy number (median = 0.321, average ± SD = 0.384 ± 0.196) was significantly lower than in 18 other brain regions.

In addition to these statistical differences, there were significant differences between caudate putamen–medial (CP-m) (median = 0.594, average ± SD = 0.567 ± 0.236) or habenular nucleus (Hb) (median = 0.325, average ± SD = 0.408 ± 0.284) and anterior amygdaloid complex–lateral (A Amy-l) (median = 1.31, average ± SD = 1.36 ± 0.48) or motor cortex–intermediate layers (Motor-in) (median = 1.31, average ± SD = 1.33 ± 0.40).

No significant differences were detected between other brain regions.

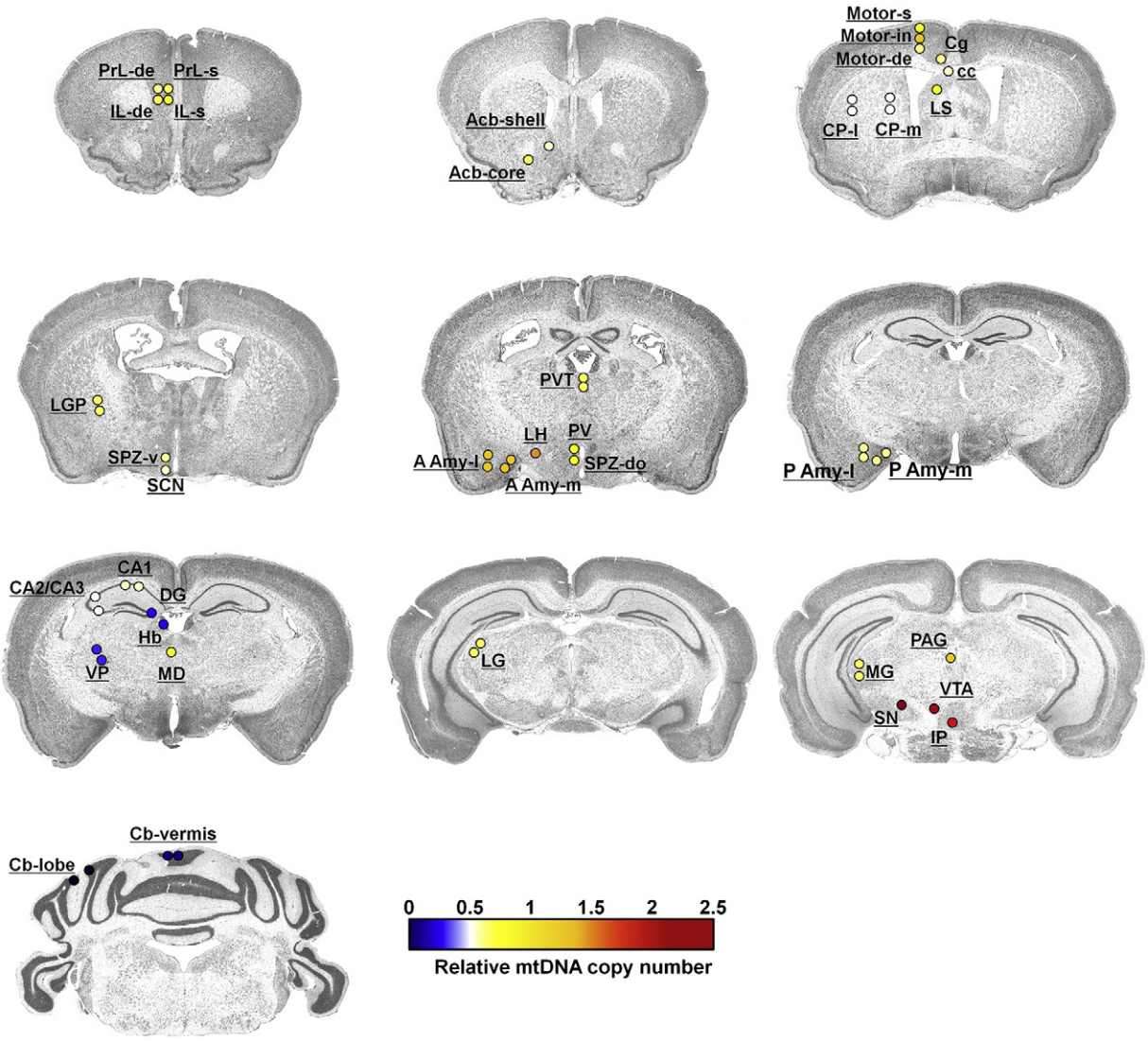

Fig. 1. Thirty-nine representative brain structures punched out bilaterally are shown in Nissl-stained coronal slices of a mouse brain. Regional variation of mitochondrial DNA (mtDNA) copy number is shown as a pseudo-color heat map. Abbreviations are expanded in Table 1.

4. Discussion

In this study, we first quantitatively demonstrated that there is a large regional variation in mtDNA copy number in the brain. Study results could be affected by regional variation in the neuron/glia ratio, if there is a difference in mtDNA copy number between neuron and glia. An *in situ* mtDNA hybridization study showed stronger signals from gray matter than from white matter in striate cortex of primates [12], and an *in situ* PCR study also showed stronger signals from neurons than from glial cells [13]. However, a study using qPCR analysis showed no statistically significant difference in mtDNA copy number between gray matter and white matter of human postmortem brains [14]. In addition, the mtDNA copy number in corpus callosum, containing mostly glial cells, was comparable to that in other brain regions in this study. The results of these quantitative analysis studies suggest that the 30-fold difference in mtDNA copy number between VTA and cerebellum cannot be solely accounted for by regional variation in neuron/glia ratio.

The highest mtDNA copy numbers were observed in VTA and SN, two major midbrain nuclei containing dopaminergic neurons. This finding might be relevant to the fact that mitochondrial dysfunction and mtDNA mutations are implicated in PD, caused by degeneration of dopaminergic neurons of SN [2,3,15]. PD is also a frequent complication of mitochondrial diseases [4,5]. Degeneration of VTA neurons is reported to be associated with depression [16], which is also a frequent comorbid condition of mitochondrial disease [5]. It remains unclear why VTA and SN contain particularly high copy number of mtDNA. It is plausible that vulnerability of mtDNA to oxidative stress resulting from the metabolism of dopamine in these two nuclei may be relevant to the present finding [17]. Meanwhile, it has recently been shown that high mtDNA copy number induces increased mtDNA deletion formation, which might be caused by increased mtDNA replication [18]. If high mtDNA copy number in SN indicates faster turnover, it might be relevant to the fact that SN is particularly susceptible to defects of the clearance of damaged mitochondria, due to mutations of Parkin and PINK1 [5,19,20].

On the other hand, cerebellar vermis and lobes had particularly low levels of mtDNA. The significantly lower mtDNA copy number in cerebellum is consistent with other reports that cerebellum showed lower level of mtDNA copies than several brain areas of rat or human [21,22]. A number of mitochondrial diseases associated with mtDNA depletion and mutations affect the cerebellum [4,5,23]. Although it is still unclear that both the regions with high mtDNA copy number such as SN and those with low copy number such as cerebellum are relevant to mitochondrial diseases, it would coincide with the fact that both depletion and increased copy number of mtDNA are reported to cause mitochondrial dysfunction [8,18]. It seems reasonable that mutation of

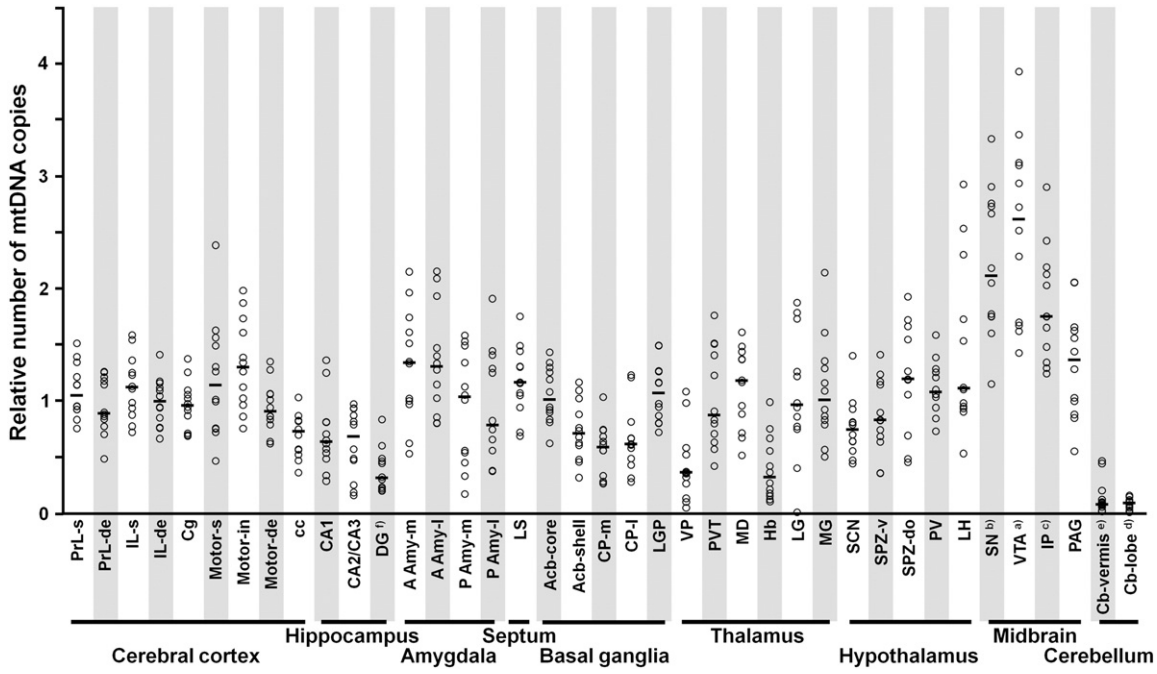

Fig. 2. Analysis of mtDNA copy number in 39 micropunched brain regions shows substantial regional variation. Each circle indicates one mouse ($n=12$). The vertical axis represents the estimated relative number of mtDNA copies to a median value of 39 brain regions. Group median values are indicated by horizontal bars. The horizontal axis represents each brain region. Differences among brain regions were observed (Kruskal–Wallis test, $P<4.8\times10^{-35}$). A multiple comparison using the Steel–Dwass test ($\alpha=0.05$) showed significant differences in mtDNA copy number among brain regions, as follows: (a) VTA > PrL-s, PrL-de, IL-s, IL-de, Cg, Motor-de, cc, CA1, CA2/CA3, DG, P Amy-m, Acb-core, Acb-shell, CP-m, CP-l, LGP, VP, MD, Hb, SCN, SPZ-v, PV, Cb-vermis, and Cb-lobe; (b) SN > PrL-s, PrL-de, IL-de, Cg, Motor-de, cc, CA1, CA2/CA3, DG, P Amy-m, Acb-shell, CP-m, CP-l, VP, Hb, SCN, SPZ-v, Cb-vermis, and Cb-lobe; (c) IP > PrL-de, IL-de, cc, CA2/CA3, DG, Acb-shell, CP-m, CP-l, VP, Hb, SCN, SPZ-v, Cb-vermis, and Cb-lobe; (d) Cb-lobe < PrL-s, PrL-de, IL-s, Il-de, Cg, Motor-s, Motor-in, Motor-de, cc, CA1, CA2/CA3, DG, A Amy-m, A Amy-l, P Amy-m, P Amy-l, Acb-core, Acb-shell, LS, CP-m, CP-l, LGP, PVT, MD, MG, SCN, SPZ-v, SPZ-do, PV, LH, SN, VTA, IP, and PAG; (e) Cb-vermis < PrL-s, PrL-de, IL-s, IL-de, Cg, Motor-s, Motor-in, Motor-de, cc, CA1, A Amy-m, A Amy-l, Acb-core, Acb-shell, LS, LGP, PVT, MD, MG, SCN, SPZ-v, SPZ-do, PV, LH, SN, VTA, IP, PAG; and (f) DG < PrL-s, IL-s, IL-de, Cg, Motor-in, Motor-de, A Amy-m, A Amy-l, Acb-core, LS, LGP, MD, PV, LH, SN, VTA, IP, and PAG. Abbreviations are expanded in Table 1.

mtDNA in smaller copy number can affect the mitochondrial function in the brain regions having lower copy number of mtDNA.

In the present study, we fixed the tissues with 4% paraformaldehyde, because it is difficult to capture more than one region at equal conditions from a frozen or fresh brain section due to its fragility. This approach also allowed us to identify brain structures clearly; we were able to pick up all brain regions from one animal at once. Moreover, we confirmed that paraformaldehyde fixation did not affect the linearity of quantification of each PCR product ($R^2>0.91$, Supplementary Figure 2) and relative amount of mtDNA per nucleus can be compared among brain regions using fixed samples. By introducing de-crosslinking, we could measure mtDNA copy number. This methodology made it possible to describe the distribution in detail.

Our findings on regional variation in mtDNA copy number in the brain provide important information on regional differences in vulnerability to mitochondrial dysfunction.

Supplementary materials related to this article can be found online at doi:10.1016/j.bbabio.2010.11.016.

Acknowledgements

We are grateful to the staff at the Divisions of Animal Experiments and Common Instrumentations in Research Resources Center, RIKEN Brain Science Institute (BSI), for technical assistance; Ms. Mizue Kametani for the care of mice used in the study; and the other members in our laboratory for valuable discussions.

This work was supported by grants from the Laboratory for Molecular Dynamics of Mental Disorders, RIKEN BSI; a Grant-in-Aid from the Japanese Ministry of Health and Labor; and Grants-in-Aid from the Japanese Ministry of Education, Culture, Sports, Science and Technology. S.F.'s research is supported by Grants-in-Aid for Young Scientists from the Japanese Ministry of Education, Culture, Sports, Science and Technology.

References

[1] D.C. Chan, Mitochondria: dynamic organelles in disease, aging, and development, Cell 125 (2006) 1241–1252.
[2] M. Baron, A.P. Kudin, W.S. Kunz, Mitochondrial dysfunction in neurodegenerative disorders, Biochem. Soc. Trans. 35 (2007) 1228–1231.
[3] M.F. Beal, Mitochondria take center stage in aging and neurodegeneration, Ann. Neurol. 58 (2005) 495–505.
[4] S. Dimauro, G. Davidzon, Mitochondrial DNA and disease, Ann. Med. 37 (2005) 222–232.
[5] A. Suomalainen, J. Kaukonen, Diseases caused by nuclear genes affecting mtDNA stability, Am. J. Med. Genet. 106 (2001) 53–61.
[6] R.K. Bai, C.L. Perng, C.H. Hsu, L.J. Wong, Quantitative PCR analysis of mitochondrial DNA content in patients with mitochondrial disease, Ann. NY Acad. Sci. 1011 (2004) 304–309.
[7] R.K. Bai, L.J. Wong, Simultaneous detection and quantification of mitochondrial DNA deletion(s), depletion, and over-replication in patients with mitochondrial disease, J. Mol. Diagn. 7 (2005) 613–622.
[8] S. Alberio, R. Mineri, V. Tiranti, M. Zeviani, Depletion of mtDNA: syndromes and genes, Mitochondrion 7 (2007) 6–12.
[9] W.C. Copeland, Inherited mitochondrial diseases of DNA replication, Annu. Rev. Med. 59 (2008) 131–146.
[10] C. Tzoulis, M. Papingji, T. Fiskestrand, L.S. Røste, L.A. Bindoff, Mitochondrial DNA depletion in progressive external ophthalmoplegia caused by POLG1 mutations, Acta Neurol. Scand. Suppl. 189 (2009) 38–41.
[11] K. Franklin, G. Paxinos, The Mouse Brain in Stereotaxic Coordinates, Academic Press, San Diego, CA, 1997.
[12] R.F. Hevener, M.T. Wong-Riley, Mitochondrial and nuclear gene expression for cytochrome oxidase subunits are disproportionately regulated by functional activity in neurons, J. Neurosci. 13 (1993) 1805–1819.
[13] S. Melov, J.A. Schneider, P.E. Coskun, D.A. Bennett, D.C. Wallace, Mitochondrial DNA rearrangements in aging human brain and in situ PCR of mtDNA, Neurobiol. Aging 20 (1999) 565–571.
[14] A. Blokhin, T. Vyshkina, S. Komoly, B. Kalman, Variations in mitochondrial DNA copy numbers in MS brains, J. Mol. Neurosci. 35 (2008) 283–287.
[15] A. Bender, K.J. Krishnan, C.M. Morris, G.A. Taylor, A.K. Reeve, R.H. Perry, E. Jaros, J.S. Hersheson, J. Betts, T. Klopstock, R.W. Taylor, D.M. Turnbull, High levels of mitochondrial DNA deletions in substantia nigra neurons in aging and Parkinson disease, Nat. Genet. 38 (2006) 515–517.
[16] R.M. Torack, J.C. Morris, The association of ventral tegmental area histopathology with adult dementia, Arch. Neurol. 45 (1988) 497–501.
[17] B. Halliwell, Reactive oxygen species and the central nervous system, J. Neurochem. 59 (1992) 1609–1623.

[18] E. Ylikallio, H. Tyynismaa, H. Tsutsui, T. Ide, A. Suomalainen, High mitochondrial DNA copy number has detrimental effects in mice, Hum. Mol. Genet. 19 (2010) 2695–2705.
[19] O. Rothfuss, H. Fischer, T. Hasegawa, M. Maisel, P. Leitner, F. Miesel, M. Sharma, A. Bornemann, D. Berg, T. Gasser, N. Patenge, Parkin protects mitochondrial genome integrity and supports mitochondrial DNA repair, Hum. Mol. Genet. 18 (2009) 3832–3850.
[20] N. Matsuda, S. Sato, K. Shiba, K. Okatsu, K. Saisho, C.A. Gautier, Y. Sou, S. Saiki, S. Kawajiri, F. Sato, M. Kimura, M. Komatsu, N. Hattori, K. Tanaka, PINK1 stabilized by mitochondrial depolarization recruits Parkin to damaged mitochondria and activates latent Parkin for mitophagy, J. Cell Biol. 189 (2010) 211–221.
[21] T. Frahm, S.A. Mohamed, P. Bruse, C. Gemünd, M. Oehmichen, C. Meissner, Lack of age-related increase of mitochondrial DNA amount in brain, skeletal muscle and human heart, Mech. Ageing Dev. 126 (2005) 1192–1200.
[22] S.C. McInerny, A.L. Brown, D.W. Smith, Region-specific changes in mitochondrial D-loop in aged rat CNS, Mech. Ageing Dev. 130 (2009) 343–349.
[23] M. Manto, D. Marmolino, Cerebellar disorders—at the crossroad of molecular pathways and diagnosis, Cerebellum 8 (2009) 417–422.